Braid description of collective fluctuations in a few-body system

Sigmund Clausen,[1,2] Geir Helgesen,[1] and Arne T. Skjeltorp[1,2]
[1]*Institute for Energy Technology, N-2007 Kjeller, Norway*
[2]*Department of Physics, University of Oslo, Blindern, N-0316 Oslo, Norway*
(Received 2 February 1998)

A few-body system of magnetic holes is studied both experimentally and numerically. Notions from braid theory are used to describe the motion in a very compact manner. The time history of *n* magnetic holes moving in a plane is represented by an *n*-strand braid, and the fluctuations of the signed crossing number is investigated. A wide range of dynamical behavior is observed. For certain parameter values the fluctuations are highly intermittent, and there is a hierarchical ordering of the dynamics in both space and time. In this case the motion is well modeled by a one-dimensional Lévy walk. [S1063-651X(98)00910-6]

PACS number(s): 05.40.+j, 05.45.+b, 75.50.Mm, 83.10.Pp

I. INTRODUCTION

How can one most simply characterize the dynamics of systems with several moving interacting particles? It has earlier been proposed that braid theory makes a compact spatiotemporal description of the dynamics in two-dimensional systems possible [1–3]. By plotting the position of an object in space versus time, one obtains a *space-time* diagram of the motion of that object. A moving particle will generate a one-dimensional curve. Several particles in motion will generate a set of braided curves. This is a way of ''freezing'' the dynamics, and the frozen dynamical structure, the *braid*, becomes the time history of the moving particles. By investigating the topology of the braid it is possible to gain insight into the particle dynamics. Braid theory is a subfield of knot theory, and has been a rich source of insight into several areas of physics lately. For example, there has been some theoretical work by Moore who looked at the motion of *n* particles in two dimensions in general, and proved that any braid type can be realized as a set of trajectories in some dynamical system [1]. Mc. Robie and Thompson used braids to describe the intertwining of a set of phase curves $(x_i(t),\dot{x}_i(t))$ in a one-dimensional dynamical system [4]. There are astrophysical applications as well. Magnetic features on the Sun can walk randomly about each other due to the turbulent convection below the surface. Berger has shown that a braid representing the time history of these motions provide topological information about the magnetic field above the surface, i.e., in the solar corona [5]. The physical realization of using knots as a space-time description of the motion of magnetic holes was introduced by Skjeltorp [2,3]. Later, notions from braid theory have been used to obtain a symbolic description of the dynamics of magnetic holes in a rotating magnetic field [6]. Braid theory made a simple topological description of the few-body dynamics possible, and the extraction of periodic orbits was straightforward [7]. The objective of the present work is to extend some of these earlier ideas, and show how to study collective fluctuations in a system of magnetic holes by means of braid theory.

Magnetic holes are nonmagnetic voids in a magnetic fluid, and may be realized by dispersing polystyrene microspheres in a ferrofluid [8]. The magnetic holes are confined between two glass plates, and forced to move about each other by a rotating magnetic field. They interact by dipolar forces, and for low values of the driving frequency the magnetic holes line up in chains which are able to follow the rotating field. This type of behavior results in a twisting of the strands representing the trajectories of the magnetic holes in space-time. There is a competition between the magnetic dipolar forces and the viscous forces from the carrier fluid. As the driving frequency is increased due to the relatively high viscosity of the ferrofluid, the chain of microspheres has to split up into smaller chain pieces which rotate with the field for a short while. In addition, there is also a rotation of the whole collection of chain pieces as one unit in terms of a twisting of the space-time trajectories. The total twist in a braid can be found, and it is possible to extract phase portraits of the periodic modes by the braid analysis [7].

The behavior may become rather complex and aperiodic if there is not full rotational symmetry of the magnetic field. A complete mapping of the modes of motion is then nearly impossible to construct [7], and one might instead focus on some other characteristics of the braid and try to describe these in order to map out the dynamic phase behavior. One such characteristic parameter is the signed crossing number, the *writhe*, of the space-time braids plaited by the magnetic holes. In this work the time sequence of the writhe has been studied, and we show that the behavior ranges from periodic to random motion. For certain values of the parameters of the driving magnetic field the dynamics is intermittent, and a hierarchical ordering takes place in both space and time. The rotational part of the motion of the holes is then well modeled by a one-dimensional *Lévy walk*, where large fluctuations lead to a socalled *superdiffusive* behavior, i.e., an enhanced diffusion [9]. The potential for such *anomalous* diffusive behavior exists in any physical situation where there is some hierarchical ordering of the processes. This ordering can take place in both space and time, and anomalous diffusion has been shown to be intimately connected to the notion of *fractal space and time* [10,11]. Recently several authors have investigated the connection between anomalous transport and Lévy statistics. The Lévy walk describes particularly well Hamiltonian chaos such as diffusion of tracer particles in a two-dimensional flow [12], and phase diffusion in Josephson junctions [13].

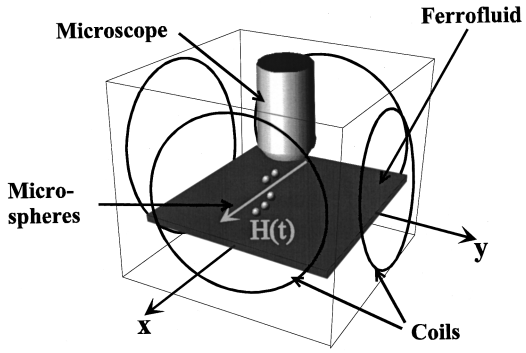

FIG. 1. Schematic view of the experimental setup with plastic microspheres submerged in a magnetized ferrofluid. Two pairs of coils are used to produce a magnetic field rotating in the (x,y) plane.

The experimental system and the model have been thoroughly discussed elsewhere [6,14,15]. A short description of our experimental system is given in Sec. II. Section III gives an introduction to braids and describes the fluctuation analysis used. The results will be presented in Sec. IV, and finally, in Sec. V, some concluding remarks will be made.

II. EXPERIMENT AND MODEL

Figure 1 shows our experimental system with magnetic holes confined by two glass plates to a nearly two-dimensional geometry. The magnetic holes consisted of monodisperse micrometer-sized spheres [16] dispersed in a magnetized ferrofluid. In the present experiment the size of the spheres used was 96 μm. A limited number of spheres could be picked out and collected by a hand held magnet when viewed in a microscope. The experimental cell was placed within a system of two pairs of coils, producing a magnetic field rotating within the sample xy plane. In order to record the motions of the microspheres we used a video camera connected to an optical microscope and a workstation to extract the positions of the microspheres. Long time sequences of the motion could be analyzed in real time, and converted into a braid notation.

When a ferrofluid sample containing monodisperse microspheres is placed in a uniform magnetic field $\vec{H}$, the voids created by the microspheres acquire an apparent magnetic dipole moments $\vec{\mu}$ antiparallel to the external field:

$$\vec{\mu} = -V\chi_{\text{eff}}\vec{H}. \tag{1}$$

Here, V is the volume of a microsphere and χ_{eff} is the effective volume susceptibility of the ferrofluid [8]. We used circularly or elliptically polarized magnetic fields rotating within the sample (x,y) plane with angular velocity ω_H

$$\vec{H}(t) = (H_x \cos(\omega_H t), \varepsilon H_x \sin(\omega_H t)) \tag{2}$$

with $\varepsilon = H_y/H_x$ as a measure of the field anisotropy.

The dipolar interaction energy of n magnetic holes of diameter d is given by

$$U(\vec{r}_1,\vec{r}_2,\ldots,\vec{r}_n,t) = \begin{cases} \displaystyle\sum_{i>j}^{n} \left\{ \frac{\mu^2(t)}{r_{ij}^3} - \frac{3[\vec{\mu}(t)\cdot\vec{r}_{ij}]^2}{r_{ij}^5} \right\} & \text{if all } r_{ij} > d \\ \infty \quad \text{if any } r_{ij} \leqslant d, \end{cases} \tag{3}$$

where $\vec{r}_{ij} = \vec{r}_j - \vec{r}_i$ is the vector joining the centres of the interacting microspheres and $\vec{r}_i = (x_i, y_i)$. The components of the magnetic force acting on the ith magnetic hole are given by

$$F_{i,\xi} = -\sum_{i>j}^{n} \frac{\partial}{\partial \xi_j} U(\vec{r}_1,\vec{r}_2,\ldots,\vec{r}_n,t), \tag{4}$$

where ξ denotes either x or y. The system is overdamped due to the large viscosity of the ferrofluid, and we may therefore neglect inertial forces. Thus, we assume that at any time the velocity of the ith magnetic hole is proportional to the force given by Eq. (4):

$$\frac{d\xi_i}{dt} = \beta F_{i,\xi}, \tag{5}$$

where $\beta = (3\pi\eta d)^{-1}$, and η is the viscosity of the ferrofluid. Equations (3)–(5) can be transformed into a dimensionless form suitable for numerical integration by letting $H_x = 1$ and $\beta = \frac{1}{6}$. By this choice of parameters, the threshold angular velocity for the stable rotation of a single pair of magnetic holes is equal to 1. The equations of motion were simulated using a fourth order Runge-Kutta algorithm, and compared with our experimental results.

For a static magnetic field the minimum energy state is reached when all the microspheres are arranged in a linear chain oriented along the direction of the field. As soon as the field starts to rotate in the plane, the chain tries to follow the rotation of the field but with a phase lag due to the viscous counterforce that slows down the motion. As long as the frequency is sufficiently low, the chain as a whole is able to follow the rotation of the field. However, above a well defined threshold frequency, the phase lag crosses a critical value and the chain may temporarily split into shorter pieces.

With the existing experimental setup it is possible to grab and digitize up to 25 images per second, which gives us a continuous motion picture of the particle dynamics. A two-dimensional projection of the (x,y,t) space-time braid traced by the motion of five magnetic holes is shown in Fig. 2(a). Due to the relatively high viscosity of the ferrofluid, the chain of microspheres has to divide into two smaller pieces containing two and three microspheres. These smaller pieces are able to rotate with the field. One magnetic hole is inter-

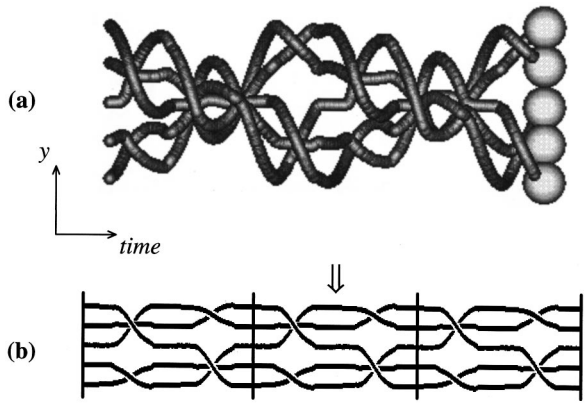

FIG. 2. (a) A space-time plot of five magnetic holes moving in the (x,y) plane. The x axis goes into the paper. (b) The resulting braid structure after removal of the total twist from the braid in (a). The periodicity is easily visible, and the repeating braid structure is indicated with the vertical bars.

changed between the two chain pieces, making the overall motion complicated. In addition, there is an overall twisting of the space-time trajectories. The total twist in the braid can be extracted by running the braid word through Garside's word algorithm [17], which can separate the external twist of an arbitrary braid from the local intertwining of the strands. Garside's solution may be given by means of *normal forms* [18]. Here we shall follow a refinement of this solution due to Elrifai and Morton [19].

Figure 2(b) shows the resulting braid structure after removal of the total twist from the braid in Fig. 2(a). The motion proves to be periodic, and it is possible to extract phase portraits of the periodic modes by this type of analysis [7]. For more complex dynamics other approaches are needed. In Sec. III we describe the fluctuation analysis of the rotational motion after a short introduction to braid theory. A more complete and thorough introduction to braid theory can be found in the book by Birman [18].

III. BRAIDS AND FLUCTUATION ANALYSIS

A geometric braid is a set of n intertwined curves stretching between two parallel planes. In order to describe a braid without having to draw it, one may decompose it into a product of elementary braids; see Fig. 3. For an n-strand system there exist $n-1$ elementary braids called generators or letters and denoted by $\sigma_1,\sigma_2,\ldots,\sigma_{n-1}$. The conventions we apply here are the following.

(i) The spatiotemporal strands traced by the magnetic holes are running horizontally from left to right, i.e., in the direction of the time axis.

(ii) The uppermost strand is denoted by 1.

(iii) An elementary braid σ_i denotes the ith strand crossing over the $(i+1)$th strand, while its inverse σ_i^{-1} denotes the ith strand crossing *under* the $(i+1)$th strand.

(iv) If none of the n strand crosses, we have an identity braid I_n.

In order to characterize the structure and complexity of a braid, different numbers or *topological invariants* can be calculated. One such number is the *writhe* of the braid, Wr, which is simply the sum of the exponents of the braid word,

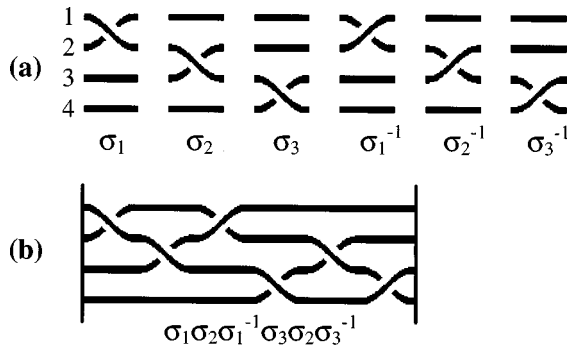

FIG. 3. The generators of the four-strand Artin braid group (a) and an example of a braid composed of them (b).

a positive crossing adds $+1$ and a negative crossing adds -1. The writhe is therefore equal to the number of positive crossings minus the number of negative crossings. As an example, consider the braid in Fig. 3(b), where $\mathrm{Wr}=2$. A second useful number to calculate is the number of *twists* in the braid. A geometric picture of a *positive half twist* of n strands, Δ_n, is obtained by imagining the n strings attached to a rod which is given a 180° twist as shown in Fig. 4. A twist commutes with all other braid structures, and therefore opposite senses of twist in a braid may be moved nearby to each other and cancel out.

For small systems of interacting microspheres under full symmetry of the driving field, the repeat period of the microsphere motion is relatively short. This makes a complete characterization of the motion in terms of a sequence of braid generators, a braid word, easy to handle. However, if the symmetry is broken as for an asymmetric, elliptically polarized magnetic field, the rotational motion is in many cases aperiodic, and one has to resort to a statistical description. There are several ways of doing a statistical analysis of braids. In the following we will show that even a simplest possible analysis of the statistical fluctuations of a braid topological invariant, like the writhe, can provide valuable information about the dynamic phase behavior.

The recipe for the fluctuation analysis is now as follows: we make a video recording of the motion of n magnetic holes, where the output is a braid word describing the space-time braid of the motion. This braid is then divided into what may be denoted *half period braids*. One half period braid is simply the space-time braid describing the motion of the microspheres during one half of the period T of the rotating field; see Fig. 5. As the total braid grows with time t, the value of Wr is extracted every time a new half period braid is plaited, i.e., whenever $t=mT/2$, where m is the number of completed half periods [20]. We set $t=m$, so that the unit of time is half a period of the rotating field. This approach results in a time series; $\mathrm{Wr}(t)$. However, this time series does not give a complete topological description of the dy-

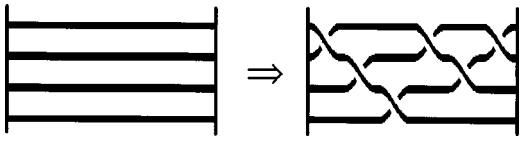

FIG. 4. A positive half twist in the four-strand Artin braid group.

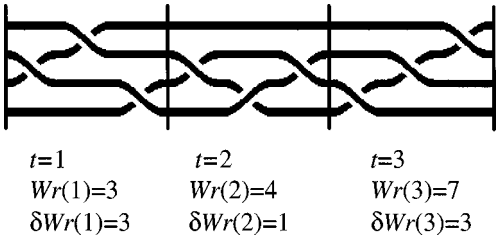

FIG. 5. Schematic illustration of the division of a braid into three half period braids. The accumulated value of the signed crossing number $\mathrm{Wr}(t)$ and the half period variations $\delta\,\mathrm{Wr}(t)$ are written below the braid.

namics, as there are several combinations of crossings of strands which result in the same value of $\mathrm{Wr}(t)$. Nevertheless, our primary goal now is to study the aperiodic motion of the magnetic holes and the fluctuations in the patterns of the strands. In addition to the total writhe as a function of time, we are also interested in the successive half period variations defined by

$$\delta\,\mathrm{Wr}(t)=\mathrm{Wr}(t)-\mathrm{Wr}(t-1), \tag{6}$$

which might be thought of as an average *writhe velocity*. $\delta\,\mathrm{Wr}(t)$ equals the writhe Wr of half period braid number t; see Fig. 5.

The maximum value which $\delta\mathrm{Wr}$ can achieve equals the number of crossings in a half twist, i.e., $(\delta\,\mathrm{Wr})_{\max}=n(n-1)/2$. This means that the motion of n magnetic holes can be described by a series of half period braids with $\delta\,\mathrm{Wr}\in[-n(n-1)/2,n(n-1)/2]$, each representing the dynamical behavior during half a period of the rotating field. The writhe velocity is a good measure of the rotational motion in the system, and a large value of $\delta\mathrm{Wr}$ indicates a high degree of rotational motion, i.e., large chain pieces are able to rotate with the field. When $\delta\,\mathrm{Wr}=(\delta\,\mathrm{Wr})_{\max}$, the whole chain of microspheres rotates in unison with the magnetic field. Since the preferred direction of rotation of the magnetic holes is in the direction of the rotating field most of the crossings of the space-time strands are positive, and $\delta\,\mathrm{Wr}>0$. However, for certain parameter values the whole chain rotates in the opposite direction to that of the magnetic field resulting in a *negative* twisting of the space-time braid [7]. The total Wr is still positive, since the smaller chain pieces rotates in unison with the magnetic field. A positive total Wr is always the case for the spatiotemporal braids in the present system.

IV. RESULTS

In the following analysis we limit ourselves to study the dynamics of $n=7$ magnetic holes. The number $n=7$ was chosen more or less arbitrarily—it is not too small ($n=2,3,4$) to make the motion relatively simple, and it is not too large ($n>10$) to make a full analysis very time consuming. However, we observe qualitatively similar statistical behavior for all n up to $n=20$ magnetic holes, which is the maximum number analyzed in this study. We fix the driving frequency to $f_H=\omega_H/2\pi=0.25$ Hz and vary the anisotropy parameter ε. Different types of dynamical behavior are observed, ranging from periodic to intermittent and random. For circularly polarized magnetic fields the motion is periodic, and the results have been described in detail elsewhere [7]. However, in order to obtain an intuitive understanding of what we do, we first illustrate the fluctuation analysis by describing how it works for the periodic case before moving on to describe more complex aperiodic dynamics. Only experimental results are presented unless stated otherwise.

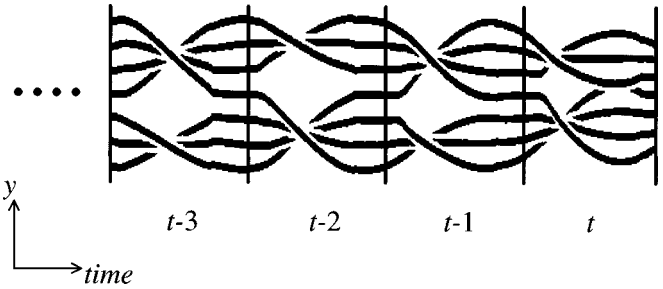

FIG. 6. Space-time braid of seven magnetic holes moving subjected to a rotating magnetic field. The field is circularly polarized ($\varepsilon=1.0$), and the motion is periodic with a slow twisting which is beginning to show.

A. Periodic behavior

For a circularly polarized field ($\varepsilon=1.0$) the solution is periodic. The frequency $f_H=0.25$ Hz is above the critical frequency $f_c\approx 0.13$ Hz for stable rotation of $n=7$ magnetic holes [7]. The linear chain of microspheres is therefore unstable, and splits into two smaller units containing three and four microspheres each; see Fig. 6. Both these units are able to rotate with the field without breaking up into smaller pieces. In addition to this internal motion, the whole chain rotates in the direction of the magnetic field resulting in a twisting of the space-time braid describing the motion of the microspheres. A careful inspection of Fig. 6 reveals a small degree of twisting. Figure 7 shows the half period variations $\delta\mathrm{Wr}$ as a function of the time t measured in units of half periods. $\delta\,\mathrm{Wr}=9$ for most of the half period braids, which is identical to the number of crossings of the strands in the half period braids. The strands of the half period braid representing the motion of the three microspheres crosses three times

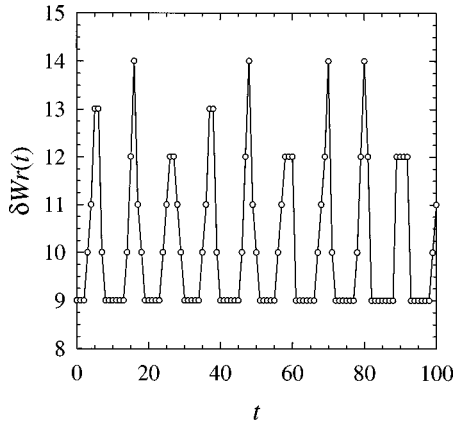

FIG. 7. Half period variations $\delta\,\mathrm{Wr}$ vs dimensionless time t measured in units of half a period of the rotating field for the mode of motion shown in Fig. 6. Lines are drawn between the points which indicate the value of $\delta\,\mathrm{Wr}$ for half period braid number t.

whereas the strands describing the motion of the four microspheres crosses six times, i.e., a total of nine crossings; see Fig. 6. In addition, the slow twisting of the braid results in higher values of $\delta\,\mathrm{Wr}$ at approximately fixed time intervals. The variations of these values of $\delta\,\mathrm{Wr}$ can be explained by the following argument: One complete half twist is usually not contained in one half period braid, and the ratio between the *average twist frequency* f_Δ and the driving frequency f_H is incommensurate. This results in some small variations of $\delta\,\mathrm{Wr}(t)$ whenever one half twist is about to be completed. However, the periodic behavior is quantified by calculating the autocorrelation function defined by

$$C(t)=\frac{\langle[\delta\,\mathrm{Wr}(\tau)-\langle\delta\,\mathrm{Wr}(\tau)\rangle][\delta\,\mathrm{Wr}(\tau+t)-\langle\delta\,\mathrm{Wr}(\tau)\rangle]\rangle}{\langle[\delta\,\mathrm{Wr}(\tau)-\langle\delta\,\mathrm{Wr}(\tau)\rangle]^2\rangle}, \tag{7}$$

where the brackets indicate averaging over all times τ, and t is a time-interval. $C(t)$ is then a measure of the spatiotemporal correlations in the system, that is, it measures the correlations between half periods braids separated by t half periods in time. Figure 8 shows the result of calculating the autocorrelation function for $\varepsilon=1.0$. A clear indication of periodic behavior is seen, where the period equals the time it takes to complete one half twist. As seen from the figure it takes about 11 half periods of the driving field before one half twist is completed, i.e., for the whole chain to complete a 180° rotation.

The motion of the seven magnetic holes is periodic and similar for all values of the anisotropy parameter down to $\varepsilon\approx0.85$. At $\varepsilon\approx0.85$ the first instability occurs, and the chain piece containing four microspheres is unstable and splits into two pairs of microspheres; see Fig. 9. However, this happens at fixed time intervals, which are equal to the time it takes to complete one half twist, that is, the previously defined period. Figure 8 shows the autocorrelation function, and the period for $\varepsilon=0.85$ is similar to that for $\varepsilon=1.0$. However, an additional peak is observed in the figure for $\varepsilon=0.85$ due to the $4\rightarrow2+2$ instability. At lower values of ε further instabilities occur and the motion becomes aperiodic.

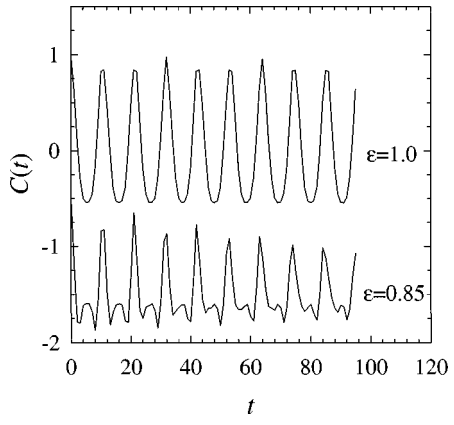

FIG. 8. Plots of the autocorrelation function $C(t)$ characterizing the half period variations $\delta\,\mathrm{Wr}(t)$ for $\varepsilon=1.0$ (upper curve) and $\varepsilon=0.85$ (lower curve). The time interval t is measured in units of half a period of the driving field. In both cases $C(t)$ fluctuates around zero, but for $\varepsilon=0.85$ the data are shifted relative to the ordinate axis for clarity.

B. Random fluctuations

As explained above, $\mathrm{Wr}(t)$ increases steadily with time t due to the large majority of positive crossings of the space-time strands. In order to observe the fluctuations more easily the average increasing trend is subtracted from the original value of $\mathrm{Wr}(t)$. The difference is denoted by $\mathrm{Wr}(t)'$:

$$\mathrm{Wr}(t)'=\mathrm{Wr}(t)-t\,\overline{\delta\,\mathrm{Wr}} \tag{8}$$

where $\overline{\delta\,\mathrm{Wr}}$ is the average value of $\delta\,\mathrm{Wr}(t)$ averaged over the total number of half periods N:

$$\overline{\delta\,\mathrm{Wr}}=\frac{1}{N}\sum_{t=1}^{N}\delta\,\mathrm{Wr}(t). \tag{9}$$

Now, for $\varepsilon<0.85$ the motion becomes aperiodic. Figure 10(a) shows $\mathrm{Wr}(t)'$ for $\varepsilon=0.80$. The associated half period variations are shown in Fig. 10(b). Figures 10(c) and 10(d) show the same quantities for $\varepsilon=0.70$. The half period variations $\delta\,\mathrm{Wr}(t)$ are still defined according to Eq. (6). Using $\mathrm{Wr}(t)'$ instead of $\mathrm{Wr}(t)$ in this definition will only shift $\delta\,\mathrm{Wr}(t)$ by $\overline{\delta\,\mathrm{Wr}}$ and the fluctuations will be centered around zero instead of around $\overline{\delta\,\mathrm{Wr}}$. For both $\varepsilon=0.80$ and 0.70, the motion of the magnetic holes was recorded for a total of 10 000 half periods of the rotating field, and the braids can then be divided into a total of 10 000 half periods braids. Only short sequences of the whole time series are shown in Fig. 10 in order to resolve the fluctuations.

Figure 11 shows the autocorrelation function $C(t)$ for the two cases. It decays exponentially with a time correlation length of about 30 half periods. This is a clear indication of random behavior with only short time correlations. In addi-

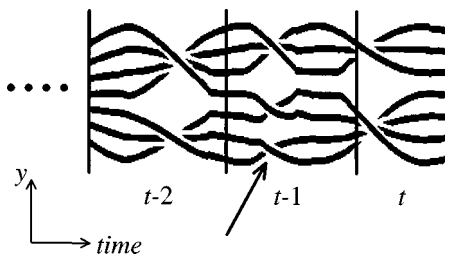

FIG. 9. The first instability of the mode of motion depicted in Fig. 6. The chain piece containing four microspheres is not stable, and divides into two smaller pieces containing two microspheres each as indicated by the arrow.

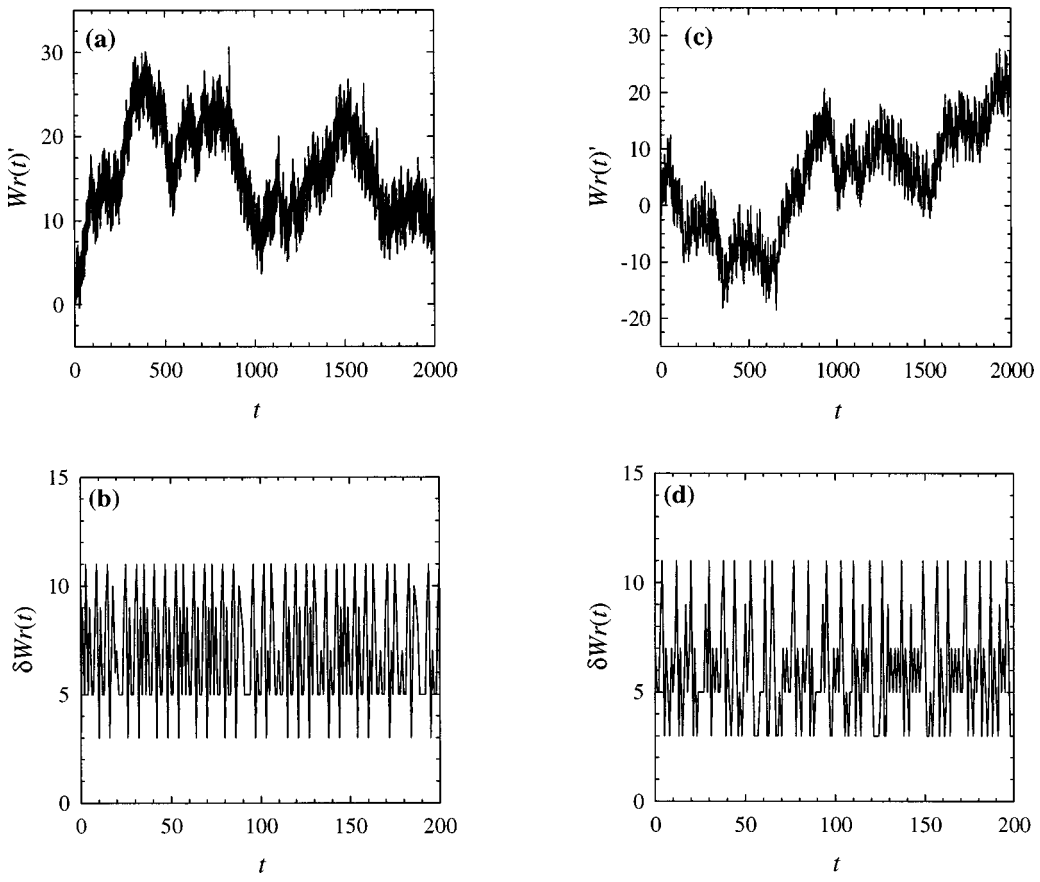

FIG. 10. (a) Time evolution of the signed crossing number $\mathrm{Wr}(t)'$ of the space-time braid describing the motion of seven magnetic holes when $\varepsilon = 0.80$. Time t is measured in units of half a period of the driving field. (b) The associated half period variations $\delta\,\mathrm{Wr}(t)$. (c) and (d) show the same quantities for $\varepsilon = 0.70$. In all four cases just a limited range of the total time series is displayed in order to resolve the fluctuations.

tion to calculating the autocorrelation function, we focus attention on the dynamics of the variations

$$\delta\,\mathrm{Wr}(t,\tau) = \mathrm{Wr}(\tau)' - \mathrm{Wr}(\tau - t)', \tag{10}$$

where both τ and t is measured in units of half a period of the rotating field. By setting $t = 1$ in this equation, one regains the definition of the half period variations in Eq. (6). It is important to notice that we select the complete set of *non-overlapping* records separated by t half periods. Varying the time interval t enables us to study the fluctuations of $\mathrm{Wr}(t)'$ on different time scales. A standard method of extracting information about the fluctuations in a time series is to calculate the variance of the successive variations in that time series. The variance of the variations defined in Eq. (10) as a function of the time interval t is given by the following expression:

$$\sigma^2(t) = \langle [\,\delta\,\mathrm{Wr}(t,\tau) - \langle\,\delta\,\mathrm{Wr}(t,\tau)\rangle\,]^2\rangle, \tag{11}$$

where the brackets indicate averaging over τ. Figure 12 shows the variance for both $\varepsilon = 0.80$ and 0.70 calculated from Eq. (11). The figure indicates random fluctuations over a relatively large time span. After an initial time span of about 30 half periods, the data approach the behavior

$$\sigma^2(t) \propto t^{1.0} \tag{12}$$

characteristic of random processes with independent increments. The deviations from the straight line in the figure for $t > 1000$ is a finite size effect due to the limited time range in the data set.

Both the autocorrelation function and the variance show a crossover from periodic to random behavior for relatively short times. The flat region in the plot of the variance for t

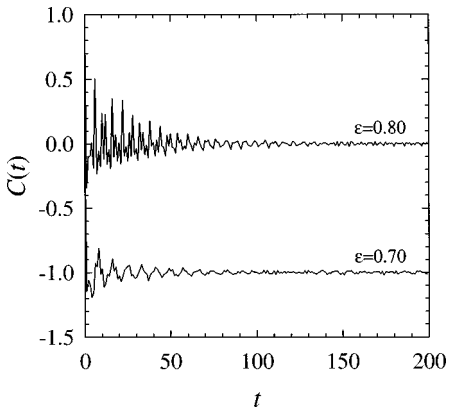

FIG. 11. Plots of the autocorrelation function $C(t)$ for $\varepsilon = 0.80$ (upper curve) and $\varepsilon = 0.70$ (lower curve). The time interval t is measured in units of half a period of the driving field. In both cases $C(t)$ fluctuates around zero, but for $\varepsilon = 0.70$ the data are shifted relative to the ordinate axis for clarity.

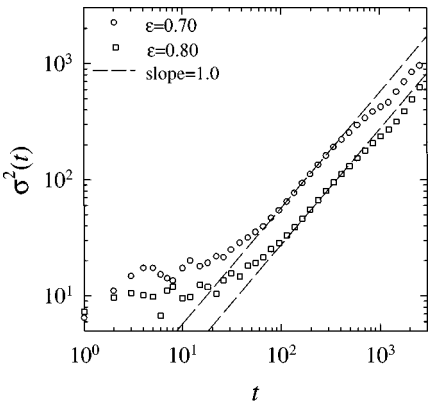

FIG. 12. Variance $\sigma^2(t)$ characterizing the increments $\delta\,\mathrm{Wr}(t,\tau)$ versus time interval t for $\varepsilon=0.80$ and 0.70. The time interval is measured in units of half a period of the driving field. The two dashed lines are the best fits to the experimental data with slopes $\eta=1.0$ in the region $t\in(50,1000)$.

<30 half periods is consistent with the short time behavior of $C(t)$. For short times the motion *appears* periodic, and the magnetic holes apparently try to find a periodic solution. Relatively many of the half period braids show a division of the whole chain into the usual two chain pieces containing three and four microspheres (Fig. 6) or a division into three chain pieces (Fig. 9). However, these solutions are only stable for short times, and the motion appears random for longer times.

C. Critical behavior, intermittency, and Lévy motion

The motion of the seven magnetic holes seems to be characterized by random fluctuations down to $\varepsilon\approx0.62$, where an interesting type of behavior is observed. At this value of the anisotropy parameter there is a finite probability for smaller chain pieces to stay separated from each other for long times. This behavior bears some resemblance to the one described earlier for two magnetic holes [21]. It was shown that when $\varepsilon<0.70$ the dynamics of two magnetic holes can be modeled by a fractal time random walk [22]. In that case the motion consists of short step rotations of the pair axis interrupted by waiting times where the two microspheres separate, and no motion of the pair axis takes place. The distribution of these waiting times shows a power law tail with an exponent depending on the magnetic field anisotropy ε. However, in the situation studied in this paper the separated chain pieces rotate with the field, and rotational motion therefore takes place during the times that they are separated. This leads to a quite different statistical behavior, and the fluctuations of the signed crossing number will be highly intermittent, and a hierarchical ordering takes place in both space and time. The separation time exponent α depends on the anisotropy parameter ε of the magnetic field, and seems to decrease with a decreasing ε. We believe that the mechanisms behind the separation of the chain pieces are similar to the mechanisms behind the separation of two magnetic holes described in detail earlier [21], but we have not been able to find any simple relationship between α and ε as was found for two magnetic holes.

The overall motion can be modeled by a continuous-time one-dimensional Lévy walk with a power law distribution of step lengths. This model of a Lévy motion was proposed by Klafter, Blumen, and Shleshinger [9]. Each time the chain of microspheres separates into smaller pieces, a new step of the random walk is started. The separation times are defined as the times the chain pieces stay separated from each other, and they are power law distributed with an exponent equal to the exponent of the distribution of the step lengths. This is always the case for a one-dimensional Lévy walk, where the velocity is independent of the step length [23].

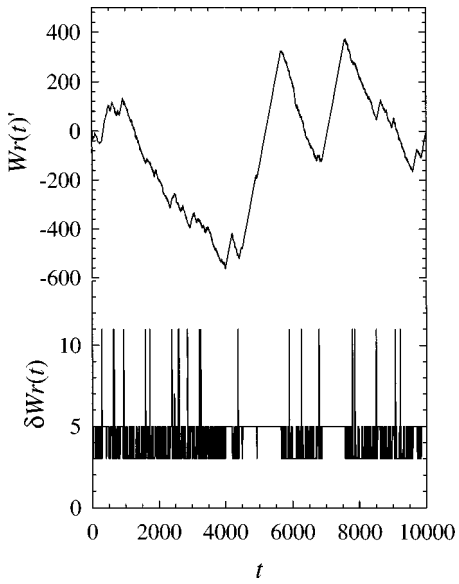

FIG. 13. Time evolution of the signed crossing number $\mathrm{Wr}(t)'$ of the space-time braid describing the motion of seven magnetic holes in an elliptically polarized field with $\varepsilon=0.55$ (upper curve). Time t is measured in units of half a period of the driving field. The lowermost curve shows the associated half period variations $\delta\,\mathrm{Wr}(t)$.

Figure 13 shows $\mathrm{Wr}(t)'$ for $\varepsilon=0.55$ with the associated half period variations $\delta\,\mathrm{Wr}(t)$ plotted below. The driving frequency is still $f_H=0.25$ Hz. The motion of the magnetic holes was recorded for 10 000 half periods of the rotating field, and the braids can thus be divided into a total of 10 000 half period braids. Clearly, the dynamical behavior differs from the one observed in the previous case. The fluctuations are much larger, and the figure also shows long steps in $\mathrm{Wr}(t)'$ with a constant velocity $\delta\,\mathrm{Wr}(t)$. There is a *distribution* of step lengths, or equivalently a distribution of time intervals where long steps in $\mathrm{Wr}(t)'$ are observed. During these long time intervals the microspheres move in a regular manner, with the chain of magnetic holes divided into three smaller pieces which rotate with the field. Two of these chain pieces contain two microspheres whereas the third one contains three, and the mode of motion is similar to the motion during the instability occurring for $\varepsilon=0.85$; see Fig. 9. The three chain pieces stay separated from each other for long times and the half period variations $\delta\,\mathrm{Wr}(t)=5$ during the steps, as seen in Fig. 13. This value equals the number of crossings of a half period braid describing $2+2+3$ magnetic holes rotating with the field. When the chain pieces are forced together again, the magnetic holes move in an aperiodic way for some time before they separate once more. The dynamical evolution is intermittent, and thus consists of both quiescent and more chaotic phases which alternate tempo-

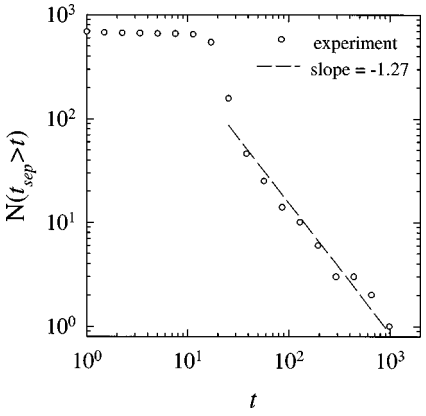

FIG. 14. Plots of the distribution $N(t_{\mathrm{sep}} \geqslant t)$ of separation times t for $\varepsilon = 0.55$. The dashed line is the best fit to the experimental data in the region $t \in (20,1000)$.

rally in an interspersed way. During the separation times the signed crossing number $\mathrm{Wr}(t)'$ increases at a constant rate causing the large scale fluctuations seen in Fig. 13. We will show that the motion is well modeled by a one-dimensional Lévy walk with a distribution $\varphi(t)$ of quiescent time intervals or separation times t. The tail of this distribution follows a power law

$$\varphi(t) \propto t^{-(\alpha+1)}, \tag{13}$$

characterized by an exponent α. The number N of separation times t_{sep} larger than t goes as

$$N = N(t_{\mathrm{sep}} \geqslant t) = \int_t^{\infty} \varphi(t_{\mathrm{sep}})\, dt_{\mathrm{sep}} \propto t^{-\alpha}. \tag{14}$$

Figure 14 shows the distribution N of separation times t extracted from the time series shown in Fig. 13. It is possible to fit the data to a power law with an exponent $\alpha = 1.27 \pm 0.13$ for $t > 20$.

We want to find out how these long tails in the distribution influence the behavior of the autocorrelation function. The experimental data of $C(t)$ in Fig. 15 is fitted to a power

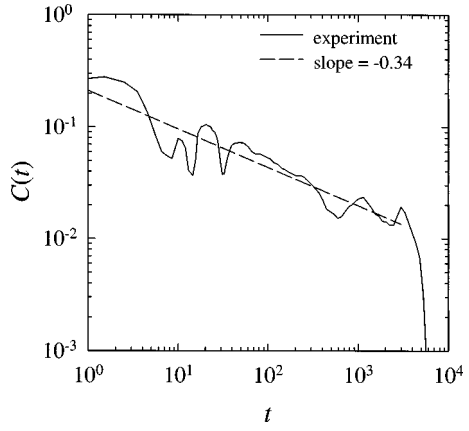

FIG. 15. Plots of the autocorrelation function $C(t)$ characterizing the successive half period variations $\delta\ \mathrm{Wr}(t)$. The time interval is measured in units of half a period of the driving field. The dashed line is the best fit to the experimental data in the region $t \in (1,3000)$.

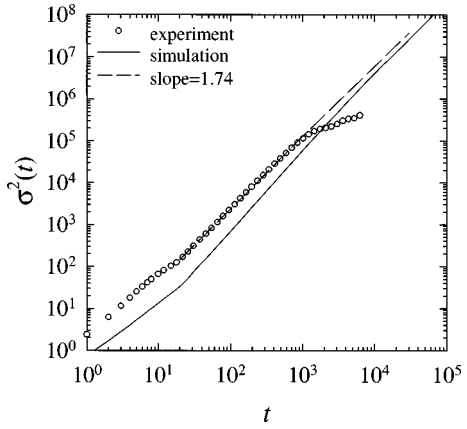

FIG. 16. Variance $\sigma^2(t)$ characterizing the increments $\delta\ \mathrm{Wr}(t,\tau)$ vs time interval t when $\varepsilon = 0.55$. The time interval is measured in units of half a period of the driving field. The dashed line is the best fit to the experimental data in the region $t \in (20,1000)$. The fitted line is extended beyond $t = 1000$ for clarity and for comparison with the numerical data (full line).

law decay over almost three decades in time, indicating long range correlations in the half period variations $\delta\ \mathrm{Wr}(t)$,

$$C(t) \propto t^{-\gamma}, \tag{15}$$

with the exponent $\gamma = 0.34 \pm 0.12$. According to theory [23], one expects $\gamma = \alpha - 1$ for a one-dimensional Lévy walk with constant velocity when $\alpha > 1.0$. This is in good agreement with our observations.

Further confirmation of the proposed Lévy motion is obtained by calculating the variance $\sigma^2(t)$ of the fluctuations of the experimental data using Eq. (11), as shown in Fig. 16. In the same figure we also display the results from a numerical simulation of the motion of the magnetic holes. In that case the dynamics was recorded for 500 000 half periods, and the parameters were the same as in the experiment. There is a good fit of the data for long times to

$$\sigma^2(t) \propto t^{\eta}, \tag{16}$$

with an exponent $\eta = 1.74 \pm 0.03$ for the experimental case. The numerical data approach the same behavior for longer times. In both cases a super diffusive behavior is observed with $\eta > 1$. As Fig. 16 shows, there is a finite size effect in the experimental data above approximately 1000 half periods, which is due to the limited time range in the data set. This observation is consistent with the results of the numerical simulation, where the super diffusive behavior extends to longer times as the length of the time series increases. The exponent η is related to the separation time exponent α by $\eta = 3 - \alpha$, when $\alpha > 1.0$ [23]. Our results are consistent with this exponent relation.

A Lévy walk is a fractal generalization of Brownian motion, and it is possible to relate the diffusion exponent η to the fractal dimension of space and time. In this simple model of diffusion, space and time are coupled, and a step in space is associated with a certain time span. The ensemble of time instants where jump events occur, form a fractal set with fractal dimension d_t:

$$d_t = \begin{cases} \alpha, & \alpha \leqslant 1 \\ 1, & \alpha > 1. \end{cases} \tag{17}$$

When do the stopover points form a fractal in space? An ordinary Brownian trajectory wiggles so much that it is actually two dimensional, independent of the dimension of the embedding space. For a Lévy walk, where $1 \leqslant \alpha < 2$, the ensemble of stopover points form a set with fractal dimension d_r [23]:

$$d_r = \frac{2}{3-\alpha}. \tag{18}$$

Thus, for the case studied here, the ensemble of stopover points form a fractal set with $d_r = 1.15$. The coupling of space and time through d_r and d_t is explicitly given by an expression for the diffusion exponent η,

$$\eta = \frac{2d_t}{d_r} = 3 - \alpha, \tag{19}$$

which is consistent with the above considerations.

V. CONCLUSIONS

Collective fluctuations in a few-body system of magnetic holes have been studied. The two-dimensional motion of n magnetic holes generates a braid in a three-dimensional space-time. By studying the fluctuations of the signed crossing number a wide range of different dynamical behavior is observed, ranging from periodic to random motion. For certain parameter values the fluctuations were shown to be highly intermittent and a hierarchical ordering takes place in both space and time. In that case the motion is well modelled by a one-dimensional Lévy walk with a power law distribution of step lengths which determines the fluctuation behavior. The dynamical evolution consists of both quiescent (regular) and more chaotic phases which alternate temporally in an interspersed way.

In conclusion, our experimental model system is simple and well defined, with precision control of all the parameters. This, coupled with computer simulations in good agreement with experiments, allows us to look for general features of nonequilibrium phenomena.

ACKNOWLEDGMENTS

This work was supported in part by the Research Council of Norway (S.C.). We want to thank A. Berge at NTNU in Trondheim, and Dyno Particles (A.S.) for kindly providing the microspheres used in these experiments.

[1] C. Moore, Phys. Rev. Lett. **70**, 3675 (1993).
[2] A. T. Skjeltorp (unpublished); also see Ref. [3].
[3] A. T. Skjeltorp, Physica A **213**, 30 (1995).
[4] F. A. Mc. Robie and J. M. T. Thompson, Int. J. Bifurcation Chaos Appl. Sci. Eng. **3**, 1343 (1993).
[5] M. A. Berger, Phys. Rev. Lett. **70**, 705 (1993).
[6] P. Pieranski, S. Clausen, G. Helgesen, and A. T. Skjeltorp, Phys. Rev. Lett. **77**, 1620 (1996).
[7] S. Clausen, G. Helgesen, and A. T. Skjeltorp, Int. J. Bifurcation Chaos Appl. Sci. Eng. (to be published).
[8] A. T. Skjeltop, Phys. Rev. Lett. **51**, 2306 (1983).
[9] J. Klafter, A. Blumen, and M. F. Shlesinger, Phys. Rev. A **35**, 3081 (1987).
[10] M. F. Shlesinger, G. M. Zaslavsky, and J. Klafter, Nature (London) **363**, 31 (1993).
[11] J. Klafter, M. F. Shlesinger, and G. Zumofen, Phys. Today **49(2)**, 33 (1996).
[12] T. H. Solomon, E. R. Weeks, and H. L. Swinney, Phys. Rev. Lett. **71**, 3975 (1993).
[13] T. Geisel, J. Nierwetberg, and A. Zacherl, Phys. Rev. Lett. **54**, 616 (1985).
[14] G. Helgesen and A. T. Skjeltorp, J. Appl. Phys. **69**, 8277 (1991).
[15] G. Helgesen, P. Pieranski, and A. T. Skjeltorp, Phys. Rev. A **42**, 7271 (1990).
[16] J. Ugelstad *et al.*, Adv. Colloid Interface Sci. **13**, 101 (1980). Produced under the trade name Dynospheres by Dyno Particles A.S., P.O.B. 160, N-2007 Lillestrøm, Norway.
[17] E. A. Elrifai and H. R. Morton, Q. J. Math. **2**, 479 (1994).
[18] J. S. Birman, *Braids, Links and Mapping Class Group*, Annals of Mathematical Study Vol. 82 (Princeton University Press, Princeton, 1974).
[19] F. A. Garside, Q. J. Math. **20**, 235 (1969).
[20] The equations of motion (3)–(5) are periodic with period $T/2$.
[21] S. Clausen, G. Helgesen, and A. T. Skjeltorp, Physica A **238**, 198 (1997).
[22] M. F. Shlesinger and B. D. Hughes, Physica A **109**, 597 (1981).
[23] X.-J. Wang, Phys. Rev. A **45**, 8407 (1992).